Integrated Aerofin/Thrust Vector Control for Tactical Missiles

Steven R. Wassom* and Lawrence C. Faupell*
Thiokol Corporation, Brigham City, Utah 84302
and
Tim Perley†
Versatron Corporation, Healdsburg, California 95448

Because of increased enemy threat and reduced defense budget, the need exists for higher performance, multiple-mission tactical missile systems. Systems studies were performed that show pulse motors and integrated aerofin/thrust vector control enhance flexibility, performance, and enable reduced-span aerofins for higher armament loading on aircraft. Trade studies resulted in the selection of a movable nozzle with an elastomeric flexible bearing and electromechanical actuators. Actuator performance requirements were determined, and actuators were designed, built, and demonstrated on bench test hardware. The actuators incorporate low-inertia brushless dc motors and a unique drive train mechanism in a low-cost, lightweight, compact package. The demonstrated performance meets the requirements of 15-deg thrust vector angle, 400-deg/s slew rate, and 45-Hz bandwidth. Development of the four-axis fin control, thermal batteries, flightweight electronics, and flexible bearing is ongoing.

Introduction

SEVERAL factors in the tactical defense arena suggest a need for the development of improved missile systems. Higher performance threats that include tactical aircraft and sea-skimming missiles call for defense missiles with extended range and more maneuverability. Budget constraints and aircraft loading limitations point to a missile with multiple-mission flexibility. Such a missile would meet the requirements of many air-to-air, surface-to-air, short-range, long-range, and high-altitude missions.

This need for improved missiles has led to advancements in solid propellant pulse motors and thrust vector control (TVC) systems. The development of these technologies has been actively pursued by both the government and private industry in a number of studies and demonstration tests.

The pulse motor serves two purposes. First, it provides a means of managing the energy and significantly enhancing missile performance and flexibility.[1-4] Figure 1 shows the target envelope of a typical 400-lb vertically launched surface-to-air missile for two different propulsion systems: a three-pulse motor and a boost-sustain motor of the same total impulse. The area of coverage is increased by about 60% with the pulse motor by optimizing the design and ignition time of each pulse. Similar advantages are available to air-launched missile systems.

The second purpose of the pulse motor is to provide thrust when needed by the TVC system to maneuver the missile under high-g requirements, such as during terminal homing. During the coast periods, the TVC is ineffectual for control, and aerofins are needed for nominal midcourse corrections. The most effective control package is known as integrated aerofin/thrust vector control (IATVC), which integrates the packaging of the TVC system with conventional four-axis aerofin control.

Trade studies to identify the principal payoffs of IATVC have shown three primary advantages:

1) The effective mission envelope is increased. Trajectory simulations were performed in which the TVC effects were modeled as an augmented autopilot time constant and an additional normal force capability. These simulations showed an enhanced ability to intercept high altitude targets, a reduced inner boundary, and the ability to engage and hit targets at aspect angles of up to 180 deg. In comparison, aero control alone was not capable of engaging rear targets. These findings are substantiated by other studies.[2,5,6]

2) The autopilot time constant is enhanced. A simulation of terminal homing was developed, and the effect of TVC on autopilot time constant was studied. These studies showed that with TVC, time constants of less than 0.2 s were achievable regardless of the size of the aerofins. Another study[2] reported similar results.

3) The fin span of the missile can be reduced. Adequate aerofin control must be available for course corrections between pulse firing, but during motor burn, the TVC provides the principal maneuvering control. A reduced fin span requirement means that more missiles can be packaged within the same allocated cross section. This is important to armament loading on both aircraft and ships.

Trade studies of various IATVC concepts have focused on the key components that drive the packaging: the thrust vectoring mechanism and the actuators. Thrust vectoring can be achieved by many different means, including movable nozzles, jet tabs, jet vanes, injection of fluid into the nozzle, etc. Jet tab and jet vane TVC systems are employed on some production missiles, but impulse losses are significant due to shock-wave inducement. Fluid injection also suffers from impulse losses as well as limited vector angles. Movable nozzles, on the other hand, are efficient and have been employed successfully on large ballistic and space launch vehicles, but have seen only isolated use on tactical missiles such as Agile,[7] with no history in a production missile. Movable nozzles were long considered too large and heavy for a tactical missile application, but recent advancements in miniature flexible bearing technology have shown the concept to be feasible. Advancements in elastomeric materials, coupled with improved design techniques that fully utilize the strain-carrying capability of the rubber, have resulted in small, lightweight flexible bearings. Figure 2 compares the size of the Agile gimballed movable nozzle and control section with a flexible bearing concept that uses elastomer pads and steel shims. This bearing design, which is in development, has been tested to a 15-deg vector angle at room temperature and to 10 deg at $-65°$F.

Actuator trade studies have been performed to identify the best type of integrated actuation system. Initially, hydraulic, pneumatic, and electromechanical (EM) systems were consid-

Received Oct. 22, 1989; revision received Feb. 15, 1990.

*Scientist. Member AIAA.
†Systems Engineer. Member AIAA.

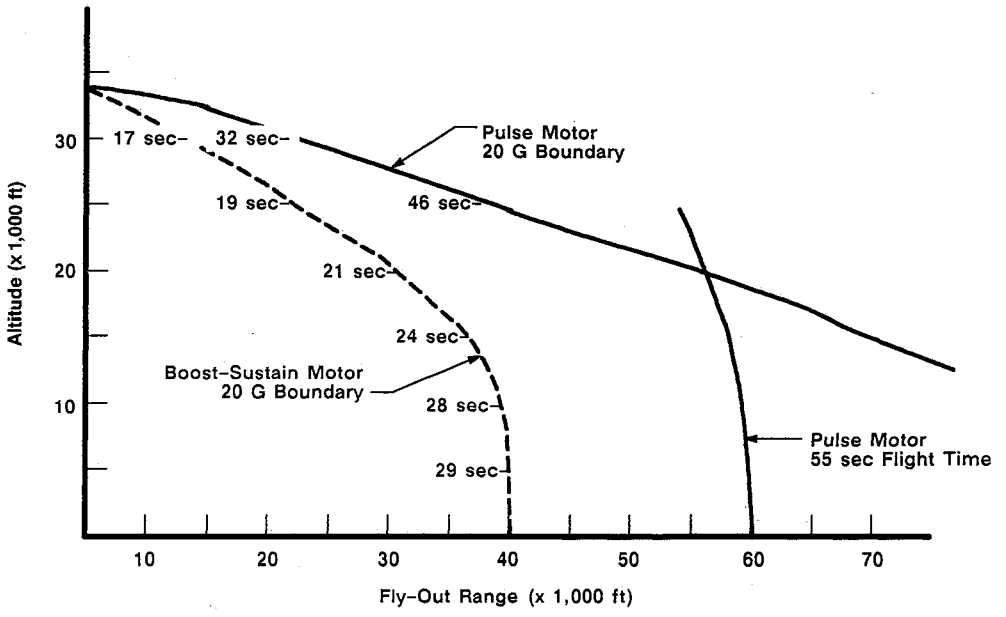

Fig. 1 Comparison of three pulse motor vs boost-sustain motor.

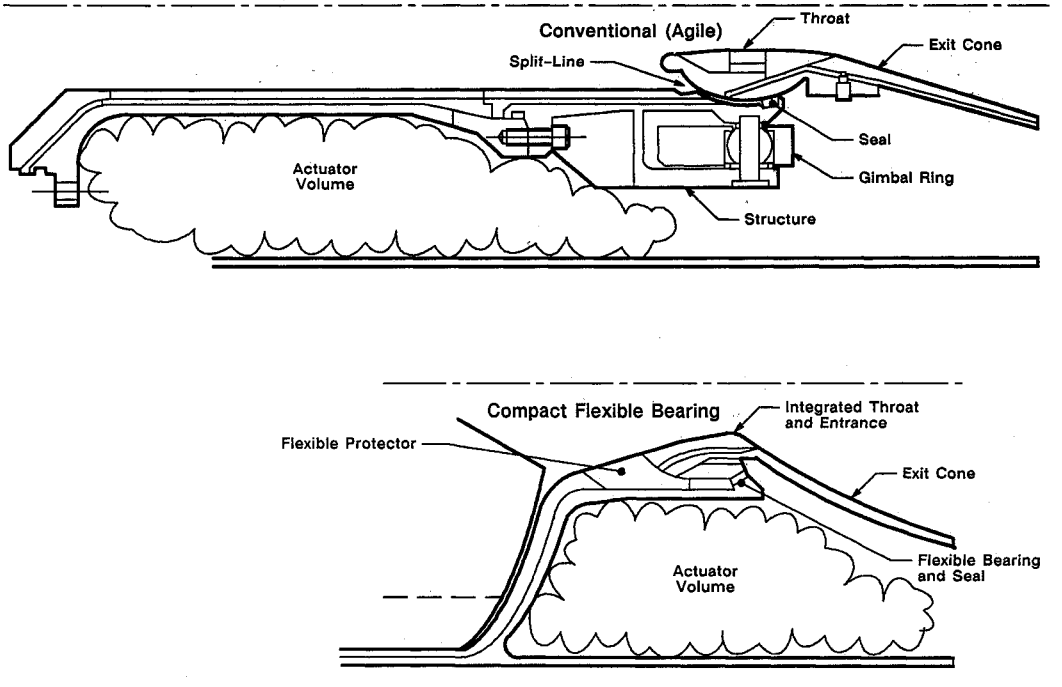

Fig. 2 Comparison of movable nozzle technology.

ered. The unique pulsed thrust feature of the missile, coupled with the desire to employ the same power source for the aerofin and TVC actuators, eliminated systems that use rocket motor chamber bleed pressure. The potentially long flight times of greater than 5 min eliminated approaches that use wasteful warm gas generators and bulky cold gas storage systems. Recent advancements in brushless dc motors, power electronics, and thermal batteries showed the electromechanical approach to be superior.

Objective

The task was divided into two parts. First, a systems analysis was to be performed to further study the advantages of IATVC and to determine the performance requirements of the actuators. Second, an integrated actuation system was to be designed, built, and demonstrated using a movable nozzle test fixture.

Systems Studies

In order to determine IATVC performance requirements and advantages, the analysis focused upon flight maneuvers that require maximum control authority. Specifically, these maneuvers included terminal target homing and the low-Q condition associated with ground launch.

Terminal Homing

The system model for terminal homing consisted of the autopilot control laws and the rigid body equations of motion for a two-dimensional horizontal plane with no roll. The mass properties and nonlinear aerodynamics came from the 8-in. missile data supplied for the High Performance/Low Observable (HP/LO) program.[5] The input to the model was the commanded g, and the output was the g achieved. The actuator dynamics were modeled as first-order lags with slew rate

and angle limits. Four autopilot gains were available to shape the transient response.

Terminal homing at both 20,000 and 70,000 ft was studied. The required velocity and g at each altitude were determined using the "rule of thumb" that a missile must be capable of achieving three times the target g-capability.[8] Assuming target maneuvering limits of 9 g at 20,000 ft and 2 g at 70,000 ft, the required velocity was found to be about Mach 1.5 at both altitudes.

Gain values were determined by linear analysis and nonlinear numerical optimization. Linearized closed-loop transfer functions were determined for the simplified cases of TVC only and aerocontrol only. Pole placement techniques were used to determine the values for the gains. These values were then adjusted in the nonlinear model to achieve the desired response.

The TVC slew rate and angle limits were varied to determine the effect on time constant at 70,000 ft. The results are plotted in Fig. 3. The points indicated as slew rate limits mark the stability boundary. For example, a time constant less than 0.16 s was not feasible with a slew rate limit of 400 deg/s because of instability. As the time constant approached the limit, the loop stability became extremely sensitive.

A maximum TVC angle requirement of 8 deg was selected since it corresponds to a "knee" in the curve in Fig. 3 and is sufficient to achieve a 0.2-s time constant. As shown in Fig. 4,[9] smaller time constants decrease the miss distance attributed to target maneuvering but amplify the effect of sensor noise. The minimum miss distance occurs near a time constant of 0.2 s. A slew rate requirement of 400 deg/s was chosen to provide a stability margin.

A TVC actuator time constant of 4 ms was selected as representative of the state of the art in EM actuator technology. Variations in the time constant did not affect the autopilot time constant noticeably.

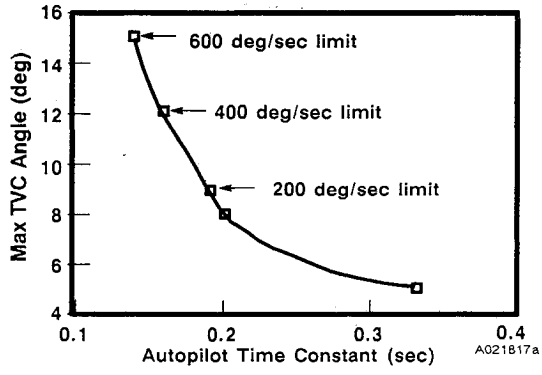

Fig. 3 Effect of TVC maximum angle and slew rate on autopilot time constant at 70,000 ft.

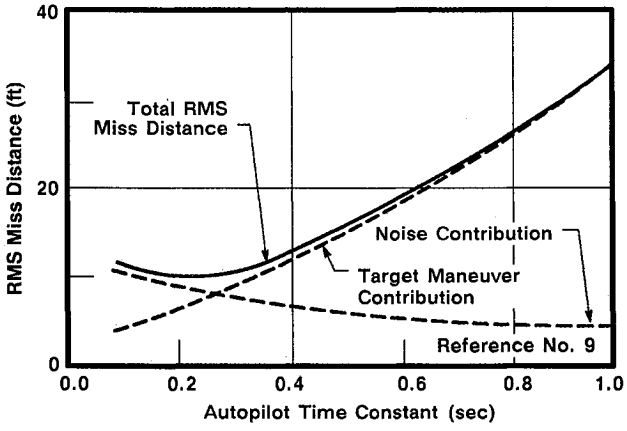

Fig. 4 Miss distance vs autopilot time constant.

An aerofin slew rate limit of 400 deg/s, an angle limit of 40 deg, and a time constant of 4 ms were selected as representative of the state of the art. The effect of aerofin control was found to be insignificant when TVC is active.

Figures 5 and 6 compare the achieved accelerations for aerodynamic fin control only vs IATVC at 20,000 and 70,000 ft, respectively. The steady-state error is due to the lack of a pure integrator in the control loop.

Several observations were made for the IATVC case:

1) Aerofin control contribution at 70,000 ft was negligible. Fin size was unimportant.

2) Some aerofin control was required at 20,000 ft in order to trim. A peak angle of 9 deg was required for full size fins. A peak angle of 2.5 deg was required for half-size fins. The difference is due to the contribution of TVC to the total trim moment.

3) The fast autopilot time constant was primarily due to the TVC. Aerofin slew rate and actuator time constant could be reduced significantly.

4) Lower angle of attack was required with TVC due to the contribution of thrust to the lateral acceleration.

5) Thrust kept the Mach number essentially constant at 20,000 ft and increased it at 70,000 ft.

6) Only one control gain required modification for the two altitudes.

Different results were observed for the case of aerofin control only:

1) Peak fin deflection angles of 25 deg were required to trim. A 40-deg transient peak was required for intercepts at 70,000 ft.

2) High slew rates (> 400 deg/s) were required to achieve the desired time constant.

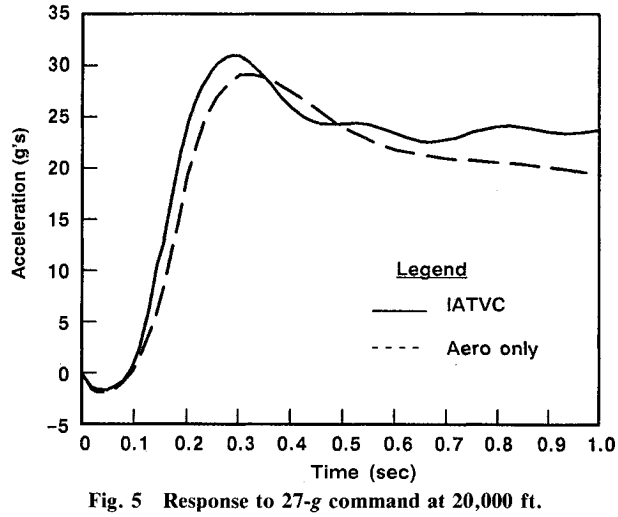

Fig. 5 Response to 27-g command at 20,000 ft.

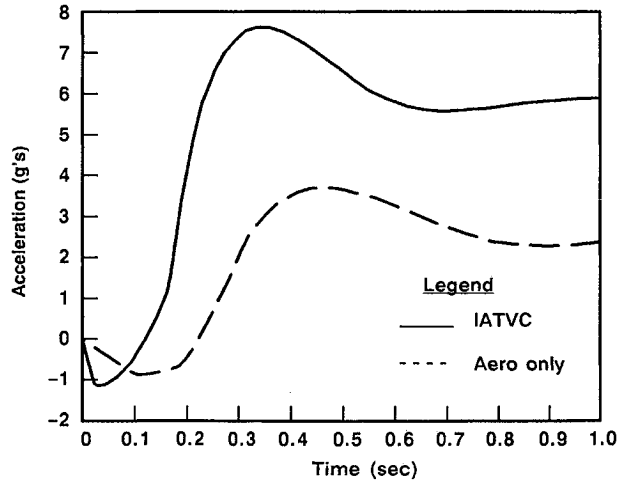

Fig. 6 Response to 6-g command at 70,000 ft.

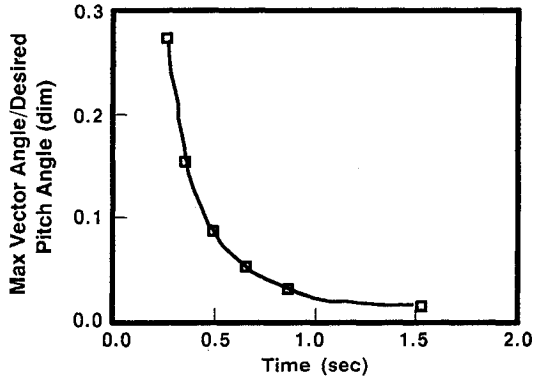

Fig. 7 Maximum TVC angle requirement for ground launch.

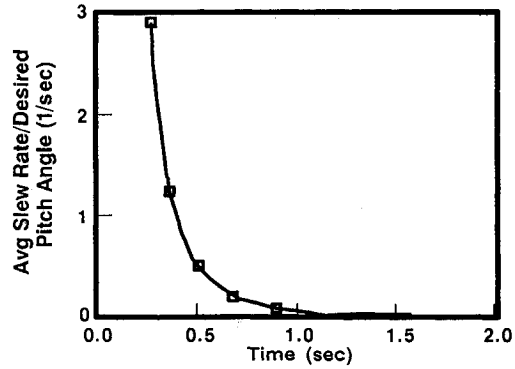

Fig. 8 TVC slew rate requirement for ground launch.

3) The terminal homing requirement of 6 g was not achievable at 70,000 ft unless the Mach number was increased by 50%.

4) All of the control gains needed modification as a function of intercept altitude.

5) Missile velocity bled off rapidly during the maneuver.

Ground Launch

Several assumptions were made in the development of a simple ground launch model for the same missile configuration used in the previous section:

1) The purpose of the IATVC system was to pitch the missile to a specified angle in minimum time.

2) Roll and yaw dynamics were neglected.

3) Since dynamic pressure is so low at and immediately following launch, missile aerodynamics were assumed to be negligible.

These assumptions resulted in a simple fourth order linear model for the pitchover maneuver. The actuator was modeled as a second order system, and the equations of motion for the body pitch dynamics were second order. Optimal linear quadratic regulator (LQR) theory was used to select the control gains to minimize the performance objective:

$$J = \int_0^\infty (R_{XX}X^2 + R_{UU}U^2)\, dt$$

The TVC angle command is represented by U, X is the actual missile pitch angle, and R_{UU} and R_{XX} are the associated weighting factors. This controller acts as a regulator which drives the missile from some initial pitch angle to a commanded zero angle while minimizing control effort and error.

The desired system dynamics were achieved by appropriately varying the weighting factors R_{UU} and R_{XX}. Parameterized curves of maximum TVC vector angle and average slew rate as functions of the desired missile pitch angle are shown in Figs. 7 and 8. The abscissa is the time required to achieve the desired pitch angle. The slew rate is based upon the time for the actuator to move from 10 to 90% of the commanded TVC angle.

Table 1 TVC and aerofin actuator requirements

Requirement	TVC	Aerofin
Deflection, deg	15	30
Bandwidth, Hz	40	45
Stall torque, in.-lb	1250	800
Slew rate, deg/s	400	600

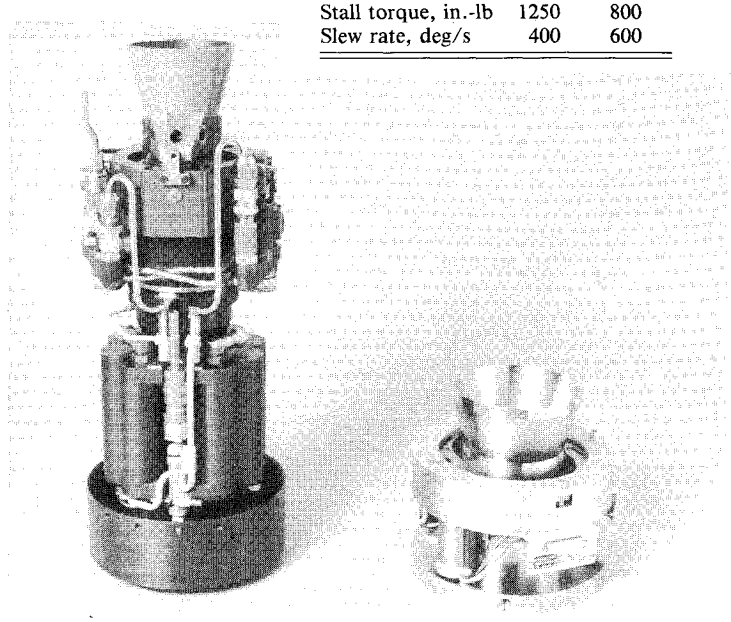

Fig. 9 Comparison of electromechanical TVC actuator (right) with Agile TVC actuator (left).

The ground launch trajectory study that resulted in Fig. 1 used a pitchover maneuver of 40 deg in 0.5 s. From Figs. 7 and 8, this requirement translates to a maximum TVC angle of about 4 deg and an average slew rate of 20 deg/s. Another ground launch study was performed on a similar missile using a complete 6-degree-of-freedom model. This missile required a roll maneuver of 180 deg simultaneously with a 90-deg pitch maneuver in 1 s, which resulted in a high TVC slew rate requirement (200–300 deg/s) to avoid introduction of excessive yaw moment.

The terminal homing requirement of 8 deg TVC angle and 400 deg/s slew rate exceeds the requirements for either of the mentioned ground launch studies. It was concluded that adequate margin exists if the terminal homing requirements are used to determine the actuator specification.

Summary of Requirements and Advantages

Table 1 summarizes the principal requirements of the TVC and aerofin actuators. The analyses above showed that a maximum TVC angle of 8 deg is adequate for the assumed 8-in. 400-lb missile configuration. However, a more ambitious goal of 15 deg was established to cover future growth requirements of various missiles. It was also shown that during motor burn the aerofin requirements can be greatly reduced. Even so, it was desired to have a system comparable to the state-of-the-art, which explains the high performance goals shown in the table. The TVC stall torque requirement is based on the predicted loads of the movable nozzle bearing. The aerofin torque requirement was derived from aerodynamic hinge moment data. The power source must be capable of operational times in excess of 300 s and of delivering intermittent peak power to the actuators. However, the studies above showed that peak power is not needed for TVC and aerofin actuators simultaneously.

Integrated Aerofin/Thrust Vector Control Mechanical Description

General

The TVC actuator is compared in Fig. 9 to the hydraulic TVC actuator of the same diameter used in the Agile missile

program.[7] Note the simplicity and compactness of the design. Although both actuators deliver similar power, the Agile actuator is more than twice as long and heavy.

The TVC actuator features a unique yoke plate mechanism and a high performance brushless motor. The motor drives the nozzle through a high efficiency spur gear drive train, as shown in Fig. 10. The yokes are close fit to the nozzle cam. During actuation the yokes pivot and push the nozzle to the desired position. Also incorporated in the system are four axes of aerofin control. The same brushless motor drives the aerofin axes through a spur gear drive train. The last pass employs a 90-deg bevel gear set.

The feedback transducers employed to close both the nozzle and aerofin loops are single turn, conductive plastic, rotary potentiometers. The position sensor for the nozzle axes is driven by the yoke pinion. The ratio between the sensor and the yoke pinion has been selected in order to achieve maximum resolution. The aerofin axes have the potentiometer mounted directly to the output shaft. Fine tuning of the nozzle null position is achieved by loosening the transducer clamps, rotating the body of the sensor, and then tightening it. The aerofin null position is fine tuned by turning an adjustment screw accessible through the fin attachment point.

Low production cost is a key design feature of tactical systems. Since the unit is manufactured entirely from standard materials and processes, the production cost of the unit is low.

Geometry

The yoke plate drive arrangement introduces some nonlinearity of travel between the yoke position and nozzle angle. Additionally, the gear ratio between the nozzle pinion and the nozzle varies nonlinearly as a function of nozzle angle. Since the nozzle is not actuated beyond 20 deg, both of these considerations can be shown to be negligible over the small angles of nozzle actuation.

The motions of the nozzle in relation to the rotational motions of the yokes are related mathematically as shown in Fig. 10. For small angles of ψ and ϕ, both triangles share the same leg x. Thus,

$$x \approx 3.75\psi \approx 2.4\phi$$

or

$$\phi \approx 1.56\psi$$

Hence, for small angles the motion is essentially linearly related.

Materials and Processes

The spur gears are fabricated using standard gear hobbing and shaping techniques from high strength precipitation hardening stainless steel. The yokes are manufactured from 6061-T651 aluminum which has been double disk ground to the required thickness and flatness. Following gear cutting, the yoke plates are treated with Teflon impregnated hard anodize to prevent galling at the nozzle cam contact. The hard coating also significantly reduces the yoke sliding friction. The housings are manufactured from 6061 aluminum as well.

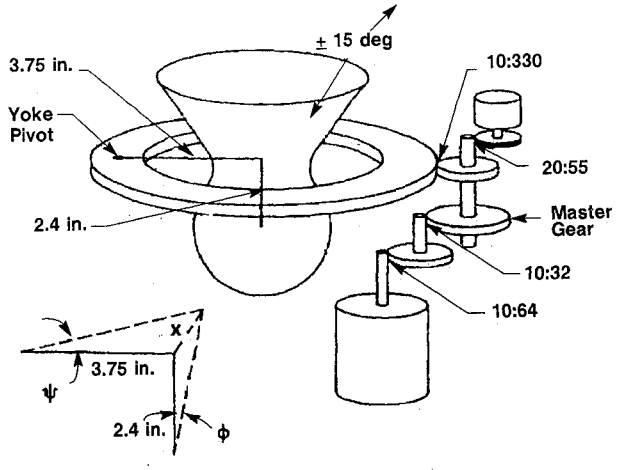

Fig. 10 Schematic of TVC actuator drive train.

The aerofin axes are manufactured using the same types of materials and processes. The gears are all high strength stainless steel, and the housings are precision machined utilizing computer numerically controlled (CNC) turning and milling.

High Performance Motor

All of the nozzle and aerofin axes are driven by the same three phase brushless motor. The motor resistance and the overall ratio between the motor and the fin axis have been optimized for the fin requirements. The key parameters of the motor are in Table 2.

The motor employs high flux density neodymium iron boron magnets in the rotor. These magnets are available in production quantities at reasonable cost. The stator laminations are stamped from low-cost silicon steel (Magnesil-N). Expensive vanadium permedur laminations have been tested, but their cost is not justified by the minor improvement in performance. The motor is commutated directly from the rotor magnetic field using hall effect sensors. The brushless design eliminates cost and reliability problems associated with graphite-silver brushes and gold plated commutators. This brushless motor can be machine wound. This eliminates the labor intensive coil insertion process typical of brushless motor manufacture. The result is a low-cost, high-reliability, high-performance brushless motor in a very small package.

Key features of the motor include its low inertia, high torque, and small size. This combination allows the servo to achieve very high performance bandwidth while driving through the 436 to 1 gear ratio of the nozzle axes or the 300 to 1 ratio of the aerofin axes. Due to the high torque-to-inertia ratio, the motor has demonstrated a no-load acceleration capability of nearly 1×10^6 rad/s^2. The motor packs a considerable amount of performance into a small volume. It is 1.5 in. in diameter and 2.25 in. long. The motor has demonstrated peak power outputs of greater than one horsepower.

Spur Gear Drive

Standard spur gears are employed in the nozzle actuators. The unique yoke arrangement results in a very high drive ratio of approximately 436 to 1. The majority of this ratio is attained between the final drive pinion and the yoke. Straight spur gears provide several advantages. First, straight spur gears are extremely efficient resulting in reduced overall power requirements and consequently smaller motor and thermal battery volumes. Second, hobbing and shaping of standard spur gears can be performed with low manufacturing costs. Third, stress analysis of spur gear drive trains is well established. Consequently, closer design margins can be tolerated with high confidence resulting in a compact, volume efficient drive mechanism with virtually no backlash.

Movable Nozzle Bearing

The movable nozzle test fixture incorporates a miniature flexible bearing (Fig. 2) with elastomer pads and steel shims. This has been bench tested to a 10-deg vector angle at − 65°F

Table 2 Motor design parameters

Parameter	Value
Motor constant, cm	0.18 in.-lb/root W
Phase-to-phase resistance	2 ohms
Stall torque	4.4 in.-lb at 15 A
No-load speed	47 KRPM at 156 V
Rotor inertia	5 E-06 in.-lb-s-s

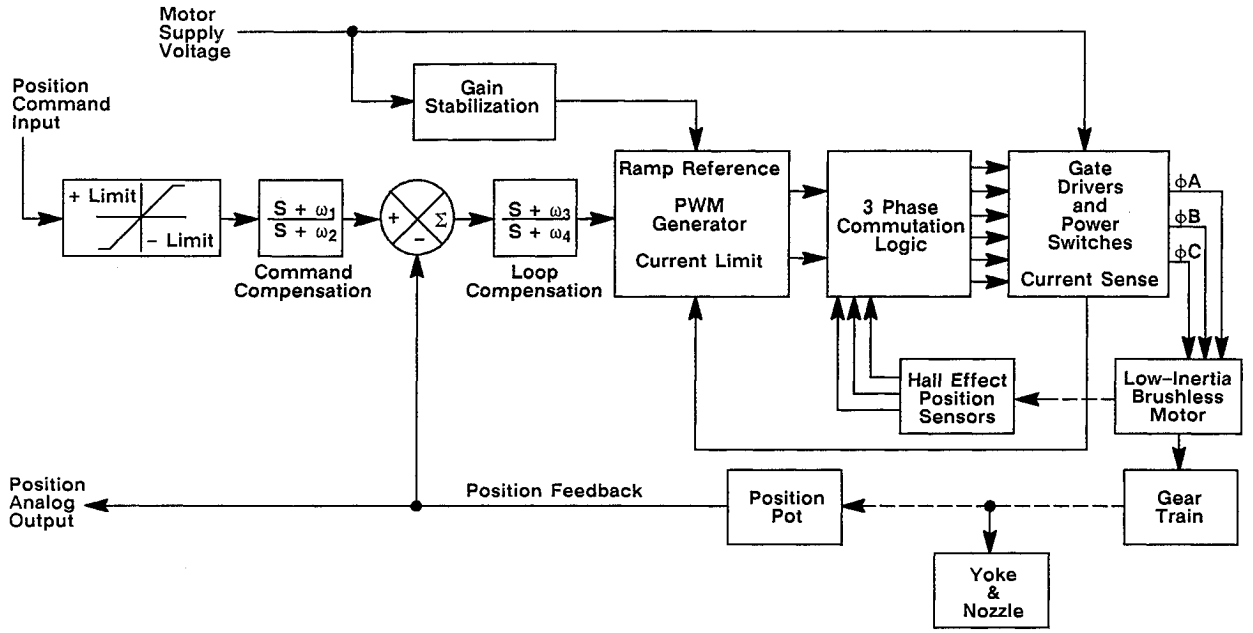

Fig. 11 Functional block diagram of motor drive circuit.

and 1000 psi chamber pressure. Vector angles of 15 deg have been achieved at higher temperatures and lower pressures. Development work is continuing to increase the pressure and vector angle at low temperature.

Integrated Aerofin/Thrust Vector Control Electronic Controller

General

A breadboard driver has been developed for this system that packages in minimum volume. Again, low production cost is one of the key objectives in the design of the servo drive electronics. As a result, the electronic circuits are composed entirely of off-the-shelf, high production, military qualified components. The electronic driver volume and component cost can be further reduced through the use of application specific integrated circuits (ASICs), programmable logic devices (PALs and EPLDs), custom resistor packs, and power hybrids. These options are currently under investigation.

Motor Drive Circuit

A functional block diagram of the drive circuit is given in Fig. 11. An integrated motor drive chip is the heart of the drive circuit. This integrated circuit includes an error amplifier, ramp reference generator, pulse width modulation (PWM) comparators, current limit comparator, and double pulse suppression. The error signal and a triangular wave reference signal are sent to the comparators, which output square wave signals. These signals drive the field-effect transistor (FET) bridge switches subject to the three-phase commutation logic. The current limit comparator switches the bridge off as soon as the current limit is reached. The double pulse suppression feature of the IC makes use of flip flop techniques to prevent the bridge from conducting again until the next PWM cycle. This is an important feature when driving high duty cycle loads.

This type of drive approach results in an effective motor drive voltage equal to a percentage of the available battery voltage. The percentage is determined by the bridge on time (which is a function of the error signal) divided by the total PWM cycle time. In this particular application, the total PWM cycle time is 50 μs since the ramp reference frequency is 20 kHz. Selection of the optimum reference frequency involves a tradeoff between FET switching losses and the steady-state conduction resistance.

Table 3 Thermal battery design parameters

Parameter	Value
Nominal open-circuit voltage	170 V
Operating voltage	156 V
Peak power	2.2 kW
Peak current	25 A
Nominal current	4 A
Number of batteries	2

In this system the motor has an inductance of approximately 2 mH, which keeps the current ripple at acceptable levels. The present design employs intrinsic FET diodes to conduct freewheeling currents. Proper shaping of the gate drives results in very reliable operation.

Power Switches

The motor drive bridge currently utilizes FETs, which are in a military qualified, electrically isolated, hermetically sealed package. These power switches have proven themselves in numerous switching power supplies and virtually any application where high reliability is required. The isolated package eliminates the need for additional isolating material between the device and the heat sink, thereby improving the thermal efficiency and reducing current drain capacitance. A similar FET package has been implemented in the breadboard as well in a plastic, commercial quality, four-dollar equivalent of the fifty-dollar fully military qualified package. Power hybrids are under consideration.

Loop Closure

This high performance servo loop is closed with simple proportional feedback only. Rate feedback is not required. Sufficient damping is inherent in the system, due mainly to the high torque-to-inertia ratio of the motor. Elimination of the tachometer and its associated demodulation electronics significantly reduces the cost and the volume of this integrated package. The position sensors are standard production potentiometers. Provisions have been made for the incorporation of command and error compensation in the form of simple lead-lag networks. Presently the loops are closed without the use of these dynamic compensation techniques. High gain and loop stiffness result in excellent frequency response and little steady-state error under loading. The gain of the loop is limited by the system nonlinearities introduced by bearing frictions, yoke to nozzle stiction and friction, and gear backlash.

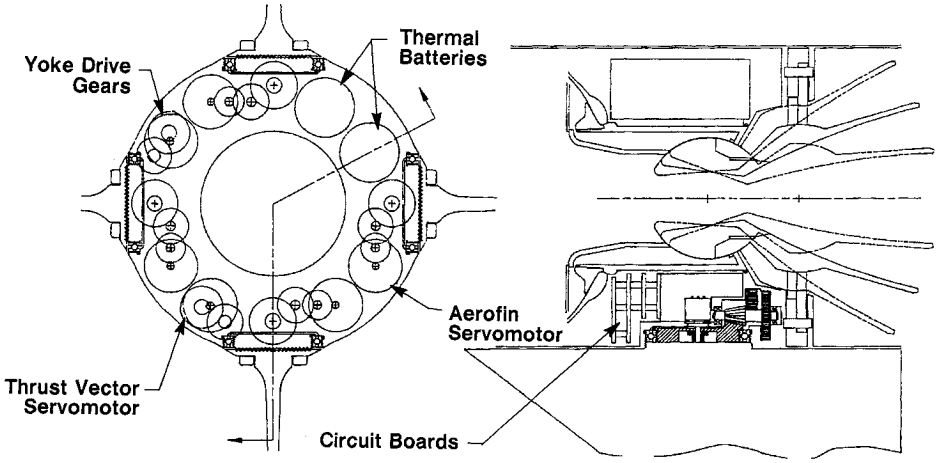

Fig. 12 IATVC actuation system packaging.

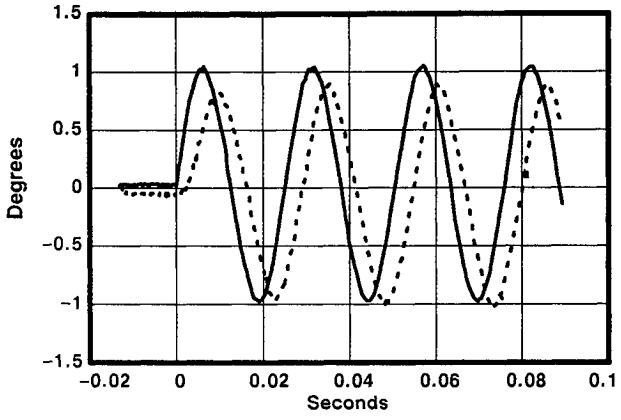

Fig. 13 TVC actuator command and response for ±1-deg sine input at 40 Hz.

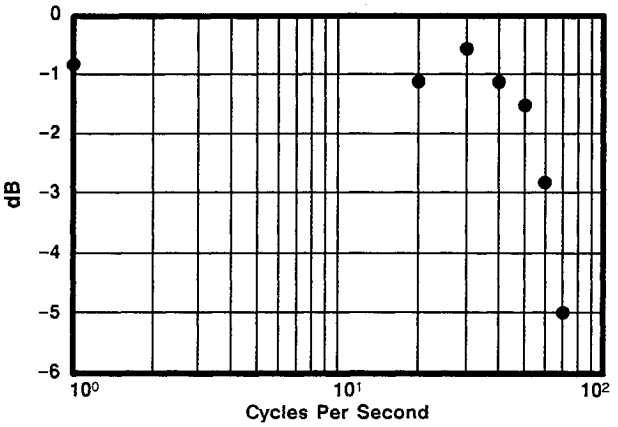

Fig. 15 TVC actuator magnitude response to ±1-deg sine input.

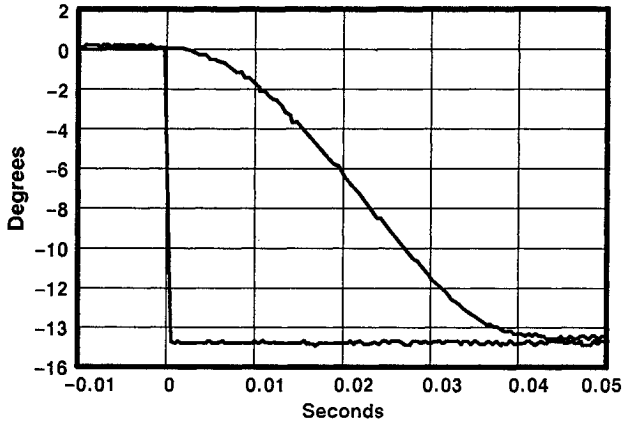

Fig. 14 TVC actuator command and response for −15-deg step command.

A unique gain stabilization feature has been employed that compensates for battery pulldown under load. This feature monitors the available bus voltage and increases the gain of the loop if the battery voltage sags. Since thermal batteries characteristically have internal impedances of 1-2 ohms, gain stabilization is particularly important for multiple axis use of the same thermal battery.

Integrated Aerofin/Thrust Vector Control Power Source

The proposed power source is a lithium disulfide thermal battery. Thermal battery technology has advanced rapidly over the past several years. These batteries supply considerable current densities and energy content. The basic parameters of the thermal batteries required for this application are in Table 3.

Battery sizing is driven in this application by the peak power requirements and not the 300-s duty cycle. Thermal battery voltage is increased by stacking cells in series and is therefore proportional to the length of the cell stack. Battery current capability increases as a function of the cell area. Consequently the current increases as a function of the cell diameter squared. Using these two guidelines, the peak power requirement is best met by a battery that fills the available annular space and whose length is then established to meet the peak power requirement with the required margins.

Integrated Aerofin/Thrust Vector Control

The system is packaged as shown in Fig. 12 in an 8-in.-diam envelope. The TVC and aerofin axes share a common mechanical housing. All six motors are essentially identical. All of the required electronics package neatly in the volume ahead of the actuator and behind the rocket motor. The length of the control section is governed largely by the required thermal battery length. The package is very compact and volume efficient. The projected weight of the complete flightweight package, including batteries and electronics, is 17 lb.

Demonstrated Performance

Typical TVC actuator performance using a heavyweight electronic driver is shown in Figs. 13 and 14. Servo frequency response is summarized in Figs. 15 and 16. These responses are essentially identical for single- and dual-axis TVC operation. To date, the nozzle actuator has demonstrated performance which exceeds the established specification. Performance of

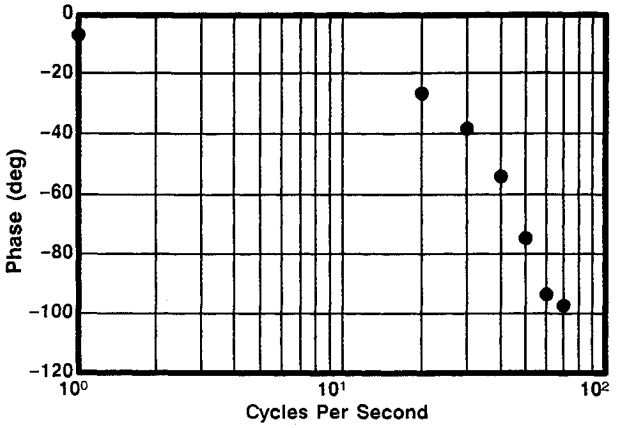

Fig. 16 TVC actuator phase response to ±1-deg sine input.

the aerofin actuators, thermal battery, and flightweight electronics will be demonstrated in the near future.

Conclusions

The systems studies reinforced the conclusions that IATVC enhances the autopilot response and allows for reduced-span aerofins. It was also concluded that aerofin actuator performance can be significantly reduced during motor burn because the TVC provides the primary control authority. The control law can be simplified for TVC because only one gain requires modification as a function of altitude. Also, TVC allows for a lower Mach number at intercept, which may translate into more range.

From the hardware demonstration, it was concluded that the actuator performance requirements can be met with the proposed EM system. Main features are an innovative yoke plate drive mechanism and the latest technology in movable nozzles, brushless dc motors, and thermal batteries. Low production cost is a feature of the motor, gear train, and electronic controller. The system packages in roughly half the weight and volume of existing systems such as Agile.

References

[1]Menon, P. K. A., Cheng, V. H. L., Lin, C. A., and Briggs, M. M., "High-Performance Missile Synthesis with Trajectory and Propulsion System Optimization," *Journal of Spacecraft and Rockets,* Vol. 24, Nov.-Dec. 1987, pp. 552-557.

[2]Froning, H. D., Jr., "Investigation of Pulse Rockets and Thrust Vector Control," Air Force Rocket Propulsion Lab., Edwards AFB, CA, AFRPL TR-86-012, Sept. 1986.

[3]Wassom, S. R., and Gunderson, R. W., "Optimal Pulse Motor Control," AIAA Paper 89-0383, Jan. 1989.

[4]Wassom, S. R., and Prows, S. R., "Application of Pulse Motors to Tactical Missiles," 1989 JANNAF Propulsion Meeting, Cleveland, OH, May 1989.

[5]Nance, P. D., "High Performance/Low Observable Motor," Vol. I, Air Force Astronautics Lab., Edwards AFB, CA, AFAL-TR-87-110, Aug. 1988.

[6]Froning, H. D., Jr., "Follow-On Investigation of Pulse Rockets and Thrust Vector Control," McDonnell Douglas Astronautics Co., Huntington Beach, CA, Paper MDC-H2108, July 1986.

[7]Voris, C. R., "Final Development Report: Agile Mod 1 Propulsion System," Naval Weapons Center Contract N00123-73-C-0400, Thiokol Corp., Brigham City, UT, Confidential Rept., March 1975.

[8]Jerger, J. J., *Systems Preliminary Design,* Van Nostrand, Princeton, NJ, 1960, p. 224.

[9]Nesline, F. W., and Nesline, M., "How Autopilot Requirements Constrain the Aerodynamic Design of Homing Missiles," Raytheon Missile Systems Div., Bedford, MA, Paper P2125, June 6-8, 1984.